SIMULATION ON THE DEFORMATION OF SURROUNDING ROCK IN FULLY MECHANIZED TOP COAL CAVING FACE IN THICK LOOSE SEAM

by

Fei LIU [a*], ***Guang-Heng GE*** [b,c], **and *Peng GONG*** [b,c]

[a] School of Resources and Civil Engineering, Suzhou University, Suzhou, China
[b] State Key Laboratory for Geo-Mechanics and Deep Underground Engineering, China University of Mining and Technology, Xuzhou, China
[c] School of Mechanics and Civil Engineering, China University of Mining and Technology, Xuzhou, China

Original scientific paper
https://doi.org/10.2298/TSCI2502123L

Based on the on-site production geological conditions, this paper comprehensively applies research methods such as numerical modelling and theoretical calculation deeply study the rock pressure behavior and deformation mechanism of the surrounding rock of the fully mechanized top coal caving face in thick and unconsolidated coal seams. At the same time, the deformation law and energy evolution characteristics of the coal pillar in the section are discussed, providing an important reference for the stability control of the end surrounding rock and the optimization of the coal pillar size.

Key words: *thick loose seam, extra thick seam, deformation mechanism*

Introduction

The source of mine pressure comes from the excavation activities of the surrounding rock in the stope [1, 2]. The activity rules of the surrounding rock in the stope can be specifically manifested through the mine pressure behavior, overlying rock migration, and surface subsidence characteristics. In 1981, Soviet scholar Boderac [3] conducted a study on the characteristics of mine pressure behavior in the coal fields in the suburbs of Moscow. The results showed that when caving in shallow coal seams, the dynamic load phenomenon of the support is very obvious, and the pressure on the working face is more intense. It is generally believed in foreign studies [4, 5] that roof fracture in shallow resource mining will directly cause surface subsidence, and a series of problems such as large roof rock fracture angle, fast surface subsidence speed, and severe weighting of the working face lead to difficulty in controlling the surrounding rock of the stope.

Previous research over the past 40 years has accumulated a large amount of material for shallow coal seam mining, such as mine pressure behavior, overburden migration rules, and surface subsidence characteristics, and also has rich experience in mining disaster prevention and control [6, 7]. However, in the actual mining process, due to the characteristics of thin bedrock, large deformation space of overlying rock, and severe mining disturbance in fully

* Corresponding author, e-mail: szxylf@126.com

mechanized top coal caving working faces in thick unconsolidated and extra-thick coal seams, there are still many uncertain factors in the deformation mechanism and control of surrounding rock under special geological conditions in the west, as well as in the prevention and control of mining disasters, and related research work is urgently needed.

Engineering background

The test mine is located in the northernmost part of the Jungar Coalfield in Inner Mongolia, with a typical loess plateau landform, an altitude of about 1127~1346 m, and an elevation difference of 219 m. The main mining area is Coal Seam 6#, with a buried depth of 230~260 m and an average thickness of 16 m. The dip angle of the coal seam is 0-80, and the fractures are relatively developed, belonging to a relatively stable coal seam. The geological conditions such as shallow burial, thin bedrock, and thick coal seams lead to large surface movement and deformation caused by mining, with cracks appearing on the surface and intense underground rock pressure.

Simulation scheme design

Based on the on-site geological conditions and measured data, the numerical model is established using FLAC^{3D} software. According to the research content, the model consists of two working faces, two target roadways, and one coal pillar. The final model size is long × wide × 240 m high × 120 m × 74 m, roadway size wide × height 5.5 m, respectively × 3.7 m, the entire model consists of 479520 units and 498736 nodes.

The stress boundary conditions are simulated using a 10.0 MPa overburden pressure at the top of the model, with sliding boundaries set around the model, and fixed boundaries set at the bottom. The improved Duncan-Chang constitutive model is used for the coal seam, and the Mohr-Coulomb model is used for the rock stratum. The excavation of coal seams is realized through a hollow model, and considering that the hollow model cannot effectively reflect the collapse and compaction process of the roof in the goaf, the Mohr-Coulomb constitutive model is reassigned to the goaf and reduced parameters are assigned to simulate the weakened rock mass.

The model based on Weibull distribution is calculated [1]:

$$\sigma = E\left(\varepsilon - \varepsilon_c'\right)\exp\left[-\left(\frac{\varepsilon - \varepsilon_c'}{\varepsilon_0}\right)^m\right] \tag{1}$$

The improved Duncan-Chang constitutive model and statistical constitutive model to characterize the stress-strain process of coal [1, 4]:

$$\sigma = \begin{cases} \dfrac{\varepsilon}{a + b\varepsilon + c\varepsilon^2}, & \varepsilon \le \varepsilon_x \\ E\left(\varepsilon - \varepsilon_c'\right)\exp\left[-\left(\dfrac{\varepsilon - \varepsilon_c'}{\varepsilon_0}\right)^m\right], & \varepsilon > \varepsilon_x \end{cases} \tag{2}$$

where

$$a = \frac{1}{E_0},\ b = \frac{1}{\sigma_c} - \frac{2}{\varepsilon_2 E_0},\ c = \frac{1}{\varepsilon_c^2 E_0},\ m = \frac{1}{\ln\left(\dfrac{\varepsilon_c E}{\sigma}\right)},\ \varepsilon_0 = \frac{\varepsilon_c}{\left(\dfrac{1}{m}\right)^{1/m}} \tag{3}$$

Stress evolution characteristics of fully mechanized top coal caving face

In order to study the influence of different non-coal drawing frames (0-7) on the stress distribution law of fully mechanized top coal caving face during the advancing process of fully mechanized top coal caving face in thick unconsolidated and extra-thick coal seams, the stress distribution law of 100 m in front of the face and 30 m behind the face during the advancing process of fully mechanized top coal caving face was analyzed.

As can be seen from fig. 1, the impact of different non-coal drawing frames on the stress of the working face is very small, and the stress characteristics of the working faces corresponding to the five non-coal drawing frames are similar. The stress in the working face gradually increases when the working face moves forward. Before the advancing of the working face 60 m, the stress of the working face corresponding to different non-coal drawing frames is basically the same. After the advancing of the working face 60 m, the stress of the working face corresponding to different non-coal drawing frames has a small difference. Compared to 1, 3, 5, and 7 non-coal drawing frames, the stress of the working face corresponding to 0 non-coal drawing frames is relatively small, with a maximum stress difference of about 2 MPa. At about 20 m in front of the working face, the stress in the working face increases to a peak value of about 30 MPa. Then, with the increase of the advance distance, the stress in the working face gradually decreases, and returns to the original rock stress around 60 m in advance; At 30 m behind the working face, the stress relief was significant, dropping to 0.5 MPa.

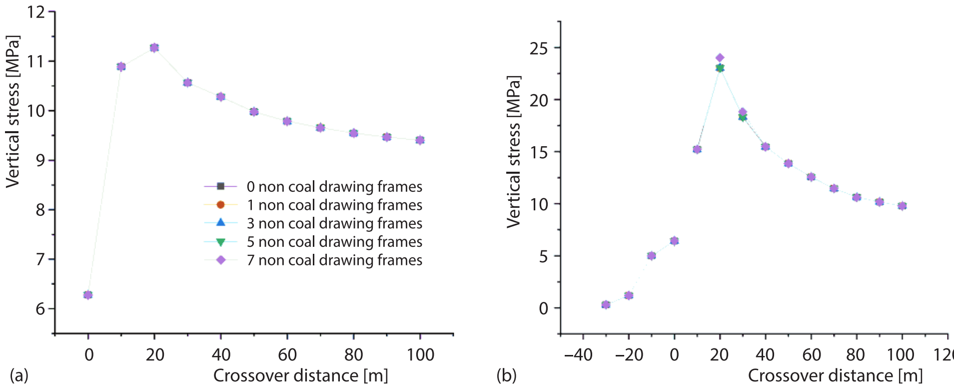

Figure 1. Stress distribution law of working face with different non-coal drawing frames; (a) advance 10 m and (b) advance 60 m

Deformation law of roadway surrounding rock

From fig. 2, with the increase of the advance distance of the working face, the subsidence amount of the roadway roof gradually decreases, and the variation trend of the subsidence amount of the roof is the same for different non-coal drawing frames. Compared to other non-coal drawing frames, the roadway roof subsidence amount is smaller when 0 non-coal drawing frames. It can be seen that at the coal wall position of the working face, the difference in roadway roof subsidence corresponding to different non-coal drawing frames gradually increases with the increase of the advancing distance, and the maximum difference reaches 200 mm when the working face advances 120 m. At 10-60 m in advance, there is a significant difference in the subsidence amount of roadway roof corresponding to different non-coal drawing frames, with the maximum difference of 1000 mm. At 60-100 m in advance, the subsidence amount of roadway roof corresponding to 1, 3, 5, and 7 non-coal drawing frames tends to be consistent, while the value corresponding to 0 non-coal drawing frames is slightly smaller, with the difference being around 50 mm.

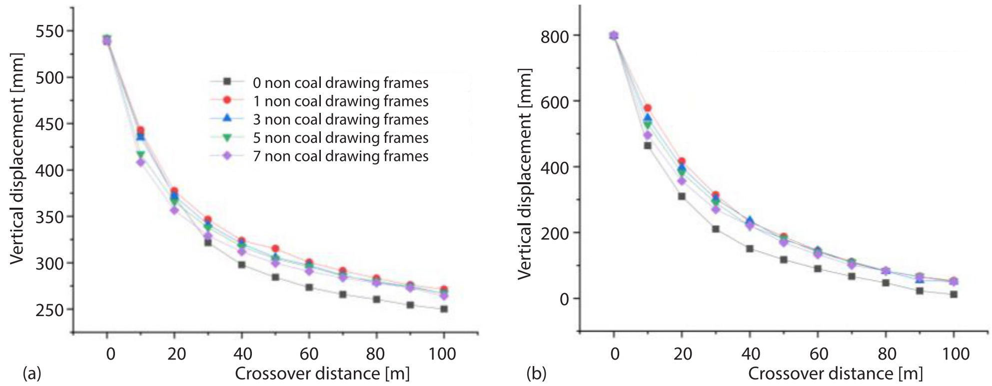

Figure 2. Displacement curve of roadway roof with different non-coal drawing frames; (a) advance 30 m and (b) advance 60 m

As can be seen from fig. 3, as the advance distance of the working face gradually increases, the displacement of the two sides of the roadway gradually decreases, and the variation trend of the displacement of the two sides is the same for different non-coal drawing frames. There is no significant difference in the displacement between the two sides of the roadway corresponding to the distance between the 3, 5, and 7 non-coal drawing frames, with the maximum difference being around 100 mm. Compared to other non-coal drawing frames, when 0 non-coal drawing frames, the displacement of the two sides of the roadway is smaller, and the difference becomes more and more obvious after advancing from the working face for 20 m. It can be seen that at a position 10 m ahead of the working face, the displacement of the two sides of the roadway corresponding to 0 non-coal drawing frames differs greatly from that of the other several non-coal caving frames, with the maximum difference reaching 700 mm when the working face advances 120 m. At an advance of 60-100 m, there is a small difference in the displacement between the two sides of the roadway corresponding to 1, 3, 5, and 7 non-coal drawing frames, and the corresponding value of the distance between 0 non-coal drawing frames is slightly smaller, with a difference of about 100 mm.

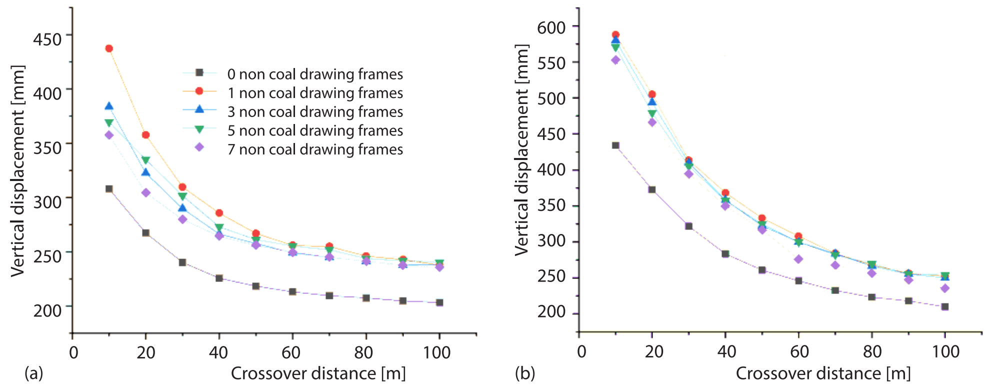

Figure 3. Approach amount of two sides of roadway with different non-coal drawing frames; (a) advance 20 m and (b) advance 60 m

Deformation and stress evolution law of coal pillar in section

Reasonable setting of coal pillars in sections is one of the key technologies for high yield and efficient production in coal mines. Therefore, the research on the reasonable size of coal pillars urgently needs to be resolved.

In order to further monitor the vertical displacement change of the coal pillar, two measuring lines are set at the horizontal direction of the 10 m coal pillar in front of the work, 7 m (Line 1) and 13 m (Line 2) from the coal pillar bottom plate. The vertical displacement change of the coal pillar is monitored, and the vertical displacement curves of the coal pillar with different sizes are obtained as shown in fig. 4.

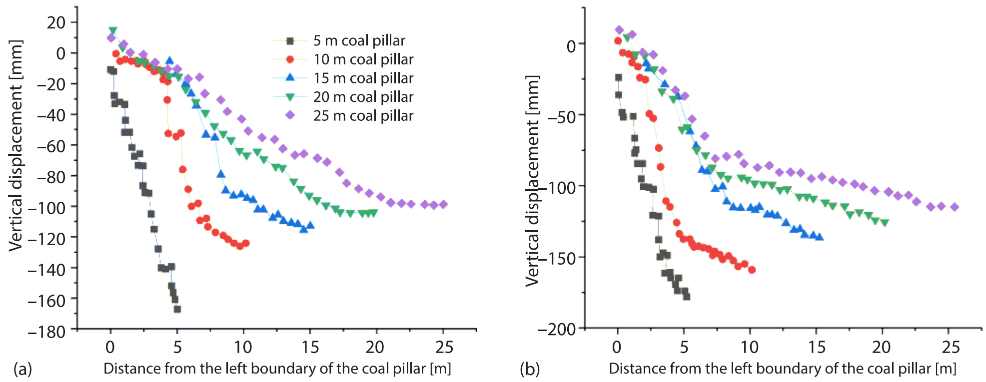

Figure 4. Vertical displacement curve; (a) Line 1 and (b) Line 2

As can be seen from fig. 4, the displacement characteristics of the two survey lines are similar, but due to the impact of mining in the working face, the displacement gradually increases as the height of the coal pillar increases. As the width of the coal pillar increases, the peak displacement gradually decreases and the survey line becomes smoother. When the width of the coal pillar is 20 m, the measuring line initially inclines, becoming smooth from 8 m away from the left wall of the coal pillar, and reaching the maximum displacement at the right wall. The peak displacement is 103 mm and 126 mm, respectively. The deformation of the coal pillar is relatively small. Compared with 20 m coal pillar, the displacement peak value of 25 m coal pillar decreases by 9.5 mm and 11 mm, respectively, with relative decreases of 4.6% and 8.7%, respectively. Compared with 15 m coal pillar, the peak displacement of 20 m coal pillar decreased by 4.7 mm and 12.3 mm, respectively, with relative reductions of 8.4% and 8.9%. Compared with 10 m coal pillar, the peak displacement of 15 m coal pillar decreases by 13 mm and 16.7 mm, respectively, with relative decreases of 10.3% and 10.8%, respectively. Compared with 5 m coal pillar, the peak displacement of 10 m coal pillar decreases by 42 mm and 25 mm, respectively, with relative reductions of 25% and 13.9%, respectively.

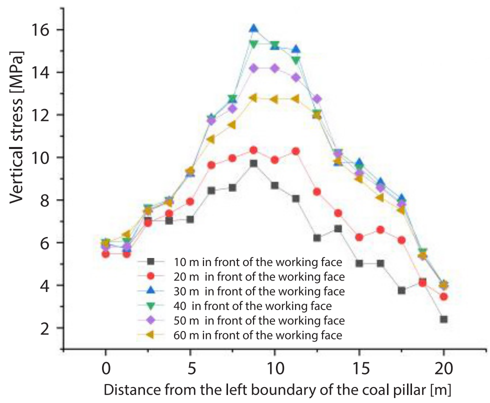

Figure 5. Vertical stress distribution law of coal pillar (20 m)

As can be seen from fig. 5, the working face is affected by advanced stress. From this, it can be concluded that the leading influence range of the working face is 20-30 m. When a 10m coal pillar is reserved, a stress peak value of 10.1 MPa occurs 30 m in front of the working face and 7.1 m from the left boundary of the coal pillar. When a 20 m coal pillar is reserved, a stress peak value of 16 MPa occurs at 30 m in front of the working face and 9 m from the left boundary of the coal pillar. In the process of advancing the working face, the peak stress of the coal pillar occurs between 9 m and 10.3 m from the left boundary of the coal pillar.

It can be seen that the stress peaks of 5 m and 10 m coal pillars are located on both sides of the coal pillar. At this time, there is no elastic core zone in the coal pillar, and almost all of them are in the plastic yield zone, which is extremely unstable. The elastic core region appeared at 15 m, but the elastic region was too narrow and still unstable; When the width of the coal pillar increases to 20 m, the coal pillar and roadway can maintain good stability. When the width of the coal pillar continues to increase to 25 m, the stress distribution characteristics have little change, achieving good roadway protection but wasting resources and lowering the coal recovery rate with excessive coal pillar size.

Conclusion

At about 20 m in front of the working face, the stress in the working face increases to a peak value, while at 30 m behind the working face, the stress relief is significant, dropping to 0.5 MPa. Compared to 1, 3, 5, and 7 non-coal caving machines, the stress in the working face corresponding to 0 non-coal caving machine is smaller, with a maximum stress difference of about 2 MPa. Compared to other non-coal drawing distances, the displacement of both sides of the roadway is smaller when 0 frame is not used for coal drawing. In comparison, when the coal pillar is 20 m long and the ends are fully drained, the double peak value of stress in the coal pillar is small, with a maximum peak distance of 12.4 m. At this time, the section coal pillar is in the most stable state.

Acknowledgment

This work is supported by Key natural science research projects in Anhui Province's universities (2023AH052244), the National Natural Science Foundation of China (52104107, U22A20598), Qinglan Project of Jiangsu Colleges and Universities, the Youth Science and Technology Talent Support Project of Jiangsu Province (TJ-2023-086).

Nomenclature

E – elasticity modulus, [GPa]
m – Duncan-Chang coefficient, [–]

Greek symbols

ε_x – axial strain, [–]
σ – first stress, [MPa]

References

[1] Xu, J., *Key Layer Theory and Its Application for Rock Movement and Control*, Xuzhou: China University of Mining and Technology, Jiangsu, China, 1999
[2] Shabanimashcool, M., Li, C. C., A Numerical Study of Stress Changes in Barrier Pillars and A Border Area in A Longwall Coal Mine, *International Journal of Coal Geology*, *106* (2013), Feb., pp. 39-47
[3] Boderac, B. B., Rock Pressure Features of Moscow Suburb Coal-Field, *Coal*, *2* (1998), pp. 1-7
[4] Missavage, J., *et al*., Subsidengce Prediction in Shallow Room and Pillar Mines, *International Journal of Mining and Geological Engineering*, *4* (1986), Mar., pp. 39-46
[5] NaPier, J. A. L., Malan, D. F., The Computation Analysis of Shallow Depth Tabular Mining Problems, *Journal of The South African Institute of Mining and Metallurgy*, *107* (2007), Nov., pp. 725-742
[6] Qian, M. G., Li, H., The Activity Law of Overlying Strata in Stope and Its Influence on Mine Pressure, *Journal of China Coal Society*, *7* (1982), 2, pp. 1-12

[7] Teng, T., Gong, P., Experimental and Theoretical Study on the Compression Characteristics of Dry/Water-Saturated Sandstone under Different Deformation Rates, *Arabian Journal of Geosciences*, *13* (2020), June, pp. 517-532
[8] Teng, T., *et al.*, Water Injection Softening Modelling of Hhard Roof and Application in Buertai Coal Mine, *Environmental Earth Sciences*, *84* (2025), 54

Paper submitted: September 1, 2024
Paper revised: October 7, 2024
Paper accepted: October 11, 2024